Materials Science for Energy Technologies 3 (2020) 91–96

Contents lists available at ScienceDirect

Materials Science for Energy Technologies

journal homepage: www.keaipublishing.com/en/journals/materials-science-for-energy-technologies

Highly sensitive and ultra-fast responsive ammonia gas sensor based on 2D ZnO nanoflakes

Srinivasulu Kanaparthi, Shiv Govind Singh *

Department of Electrical Engineering, Indian Institute of Technology Hyderabad, Kandi 502285, India

ARTICLE INFO

Article history:
Received 26 May 2019
Revised 13 October 2019
Accepted 14 October 2019
Available online 23 October 2019

Keywords:
Ammonia sensor
2D ZnO
Chemiresistive gas sensor
Environmental monitoring
Drift correction

ABSTRACT

Detecting ammonia in ambient air with high sensitivity and ultra-fast responsivity is crucial given its implications on human health. The response of such sensors should also be reversible to use them for continuous monitoring. Herein, we report a reversible ammonia (NH_3) sensor based on 2D ZnO nanoflakes at 250 °C. The sensor exhibited a maximum response of 80% and sub-15 s response and recovery times upon exposure of 0.6–3 ppm NH_3. Further, we formulated and corrected the baseline drift with a simple and straightforward baseline manipulation method. The excellent response of the sensor indicates the feasibility of using it in diverse applications where high sensitivity and rapid response are crucial.

1. Introduction

Ammonia (NH_3) is a commonly used chemical in many industries that range from agriculture to petroleum industry. NH_3 is an important source for nitrogen, which is essential for plant growth, and thus it is used as a fertilizer in the form of liquefied gas. It also acts as an anti-fungal agent and preservative in agriculture industry. Furthermore, it is used as a curing agent in leather industry, as a nitrogen source in food and beverage industry, and as an anti-corrosive in petroleum industry. However, it is one of the highly toxic gases its detection and quantification in air is vital, given its implications on human health [1–4]. As per OSHA, the acceptable limit of NH_3 at the workplace is 25 ppm for 8 h work shift [5,6]. Exposure to higher concentrations of NH_3 causes respiratory problems, and may even lead to death. Thus, the rapid detection of NH_3 in the air with high sensitivity is crucial.

Several NH_3 gas sensors based on conducting polymers [7,8], Carbon nanotubes [9], Graphene and other 2D materials [10–12] and metal oxides [13–23] have been reported in this regard. Nevertheless, these devices are weak in one or more aspects of sensitivity, response time, and reversibility, and thus, improvement is necessary to use them in the full range of practical applications. The sensors based on conducting polymers, 2D materials, and carbon nanotubes can detect ammonia gas at low temperatures. However, the sensors based on these materials suffer from the irreversible response. Moreover, they are extremely dependent on variations in ambient temperature and humidity. Temperature and relative humidity related errors can be nullified using proper algorithms if the response/recovery times are small. However, the response/recovery times of majority of low temperature sensors are in several minutes, and the temperature and relative humidity can vary during this period. On the other hand, metal oxide gas sensors working at high operating temperature exhibit reversibility as well as reasonably good response and recovery times. The only drawback associated with high temperature operation is high power consumption of the sensors. Nevertheless, significant research is going on the design of micro heaters which can reduce the power consumption.

ZnO is an n-type semiconductor, that is widely used in various applications such as sensors, biodegradable and biocompatible electronics, photo catalysis, solar cells, transparent electrodes and photodetectors [14–38]. It is an ideal material for gas sensing owing its large band gap, large binding energy, good thermal stability and high electron mobility. Moreover, it can be easily prepared at low cost and thus mass production is possible. Herein, we implemented a resistive ammonia sensor based on 2-Dimensional (2D) ZnO nanoflakes (NF). The 2D ZnO NF were prepared by the simple wet chemical method. The sensor exhibited a very high sensitivity, reversible response and low response and recovery times at 250 °C. However, the reported sensor exhibited the baseline drift which can hinder its utility in practical applications. This drift in the baseline was corrected using a simple base-

* Corresponding author.
E-mail address: sgsingh@iith.ac.ing (S. Govind Singh).
☆ Peer review under responsibility of KeAi Communications Co., Ltd.

https://doi.org/10.1016/j.mset.2019.10.010

line manipulation approach. As the performance of the sensor is excellent in many aspects, it will present numerous benefits despite its high operating temperature.

2. Experimental

2.1. Materials

Zinc acetate dihydrate ($Zn(CH_3COO)_2 \cdot 2H_2O$) and sodium hydroxide (NaOH) were acquired from Sigma Aldrich (USA). Ethyl alcohol (CH_3CH_2OH) and 2-Propanol ($(CH_3)_2CHOH$) were procured from Hychem Labs (India) and Sisco Research Laboratories (India) respectively.

2.2. Synthesis of 2D ZnO nanostructures

The 2D ZnO NFs were synthesized using precipitation method at low temperature [24]. First, 1300 mg Zinc acetate dihydrate is dissolved in 60 mL deionized water followed by the addition of 1200 mg of NaOH and stirred at 50 °C for 40 min. Next, the resultant material is washed with DI water and ethyl alcohol multiple times using a centrifuge at 3000 rpm for 10 min and dried it overnight at 60 °C to get white ZnO powder.

2.3. Material characterization

The characteristics of ZnO are investigated with X-Ray diffraction spectroscopy (XRD, PAN analytic X'pert) with a wavelength of CuKα1 (1.54 Å) in the 2θ range of 25° to 70°, Field emission scanning electron microscopy (FESEM, Zeiss) and UV–Visible spectroscopy.

2.4. Sensor fabrication and gas sensing

The chemiresistive sensor is fabricated by drop-coating ZnO dispersed in 2-Propanol. Silver paste is used for the contact electrodes. The experiment was carried out in a gas chamber by applying a 5 V power supply to the sensor and measuring the current through it using Keithley 2450 Source Measurement Unit upon exposure of the target gas with desired concentration at different operating temperatures. Dry NH_3 and synthetic air were used throughout the experiment. Mass Flow Controllers (MFCs) are used to mix them in the right proportion to get the required concentration of NH_3.

3. Results and discussions

3.1. Material characterization

To investigate the morphology of sensing material (ZnO) of the chemiresistive sensor (Fig. 1(a)), FESEM images are captured. The ZnO has a thin and planar flakes structure, as shown in Fig. 1(b). To know the crystallinity of the prepared NFs, X-Ray diffraction studies (XRD) are carried out. The XRD peaks (JCPDS No. 36-1451) (Fig. 1(c)) indicate that ZnO has a Wurtzite structure with high crystallinity. It has a crystal size of 40.71 nm with lattice constants a (3.25 Å) and c (5.19 Å). The Tauc plot plotted from absorption spectra (UV–Vis) in Fig. 1(d). depicts that the material absorbs well below 380 nm and has a band gap of 3.27 eV.

3.2. Ammonia detection with the sensor

To determine the sensing characteristics of the sensor towards ammonia, it was supplied with a voltage of 5 V and measured the response with exposure to ammonia gas. Fig. 2a shows the response ($y = R_a/R_g$, Ra: Resistance of the sensor in air, Rg: Resistance of the sensor in the presence of target gas) of the sensor upon exposure of 0.6 ppm to 3 ppm NH_3 at 250 °C. The sensor resistance decreased with the exposure of the ammonia gas, and it recovered back to the original value upon replacing ammonia with synthetic air. The response corresponding to Fig. 2a is nonlinear with the concentration of the gas as shown in Fig. 2b, and it is fitted with

$$y = y_0 + A * |x - x_c|^P \tag{1}$$

This relation is in agreement with the reported responses of the other sensors in the literature [15,39,40]. In fact, the relation between the sensor response (y) and gas partial pressure (P), which is directly proportional to the gas concentration, should be of the form

$$y = K(P)^n \tag{2}$$

where K is a pre-factor, x_c is constant, and n is an exponent. The n value is ideally 1, but it deviates from this value in this case, which may be attributed to the oxygen vacancies present in the structure. The coefficient values are mentioned in Table 1.

The responsivity or response (S) of the sensor can be determined using the Eq. (3)

$$S = \frac{R_a - R_g}{R_g} \tag{3}$$

where R_a and R_g are sensor resistances before and after the exposure of NH_3 respectively. The sensor exhibited a high response of 80% at 3 ppm NH_3 concentration. Further, the steady-state characteristics of the sensor upon exposure ammonia were analyzed at 250 °C. It exhibited a response time of 3–15 s whereas recovery time is 5–14 s as depicted in Fig. 2c. The response time (τ) of a gas sensor is

$$\tau = \left(\frac{1}{k}\right) * \left(\frac{K}{1 + P_g K}\right) \tag{4}$$

where k and K are forward, and reverse rate constants and P_g is the partial pressure of the gas [41]. As P_g is directly proportional to the gas concentration, the equation for low gas concentrations can be re-written as [42]

$$t_{r lim P_g \to 0} = lim\ P_g \to 0^{\left(\frac{1}{k}\right) * \left(\frac{K}{1 + P_g K}\right)} = \frac{K}{k} \tag{5}$$

Therefore, the sensor response time is almost constant, which is 9 s in this case with 6 s deviation.

3.3. Repeatability and baseline drift correction

To investigate the repeatability of the sensor, it is exposed to 3 ppm ammonia for 4 cycles (Fig. 3a). The sensor is fully reversible and repeatable over time with slight baseline drift in the response. This baseline drift can be attributed to various structural variations such as chemical diffusion of oxygen vacancies and degradation of electrical contacts [43–45]. We proposed a simple two-step baseline manipulation technique to correct the baseline drift of the sensor response.

(1) First, we fit the baseline (X(t)) of the sensor with a nonlinear exponential function, as shown in Fig. 3b with Eq. (6).

$$X(t) = 0.79462 * \exp(-t/1126.79) + 0.174 \tag{6}$$

(2) Next, the baseline is corrected (Y(t)) using a simple division as represented in equation (7) to get the plot in Fig. 3c.

$$Y(t) = (R/R_0)/X(t) \tag{7}$$

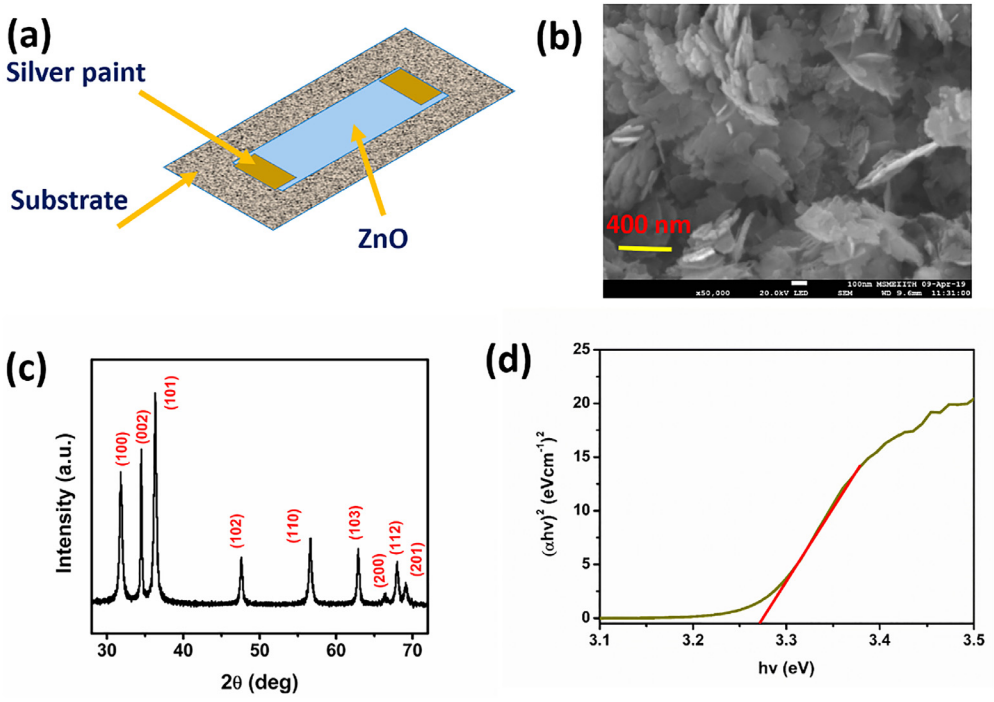

Fig. 1. (a) Ammonia sensor schematic; (b) Micrograph; (c) XRD; and (d) Tauc plot of 2D ZnO NFs.

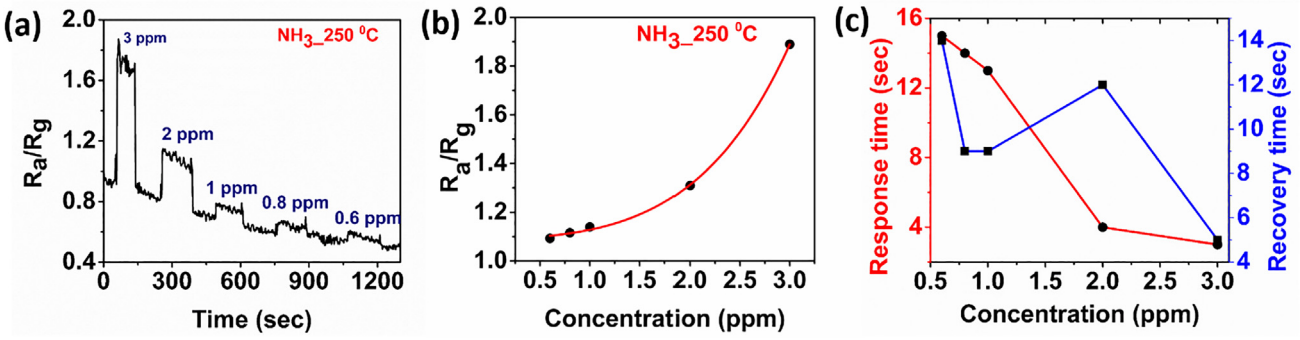

Fig. 2. (a) Response of the sensor with NH_3 at 250 °C; (b) Response of the sensor with respect to gas concentration; (c) Response/recovery times of the sensor with different concentrations.

Table 1
The coefficients of nonlinear fitting of sensor response and the response at different temperatures.

Temperature (°C)	A	P	x_c	y_0	Response (%) @ 3 ppm
250	2.19653e−4	5.28772	−1.72053	1.08483	~80
300	0.00178	3.55637	−2.1649	1.03757	~70
350	5.67785e−4	4.95405	−1.41477	1.11025	~90

It can be observed that the baseline is corrected and flat. Moreover, the response for multiple cycles is almost the same, which is the required condition for using a sensor in practical applications.

3.4. Sensor response with temperature

Further, we investigated the response of the ZnO sensor at temperatures higher than 250 °C. Fig. 4a and Fig. 4b shows the responses of the sensor at 300 and 350 °C respectively. The response of the sensor with concentration is reversible and following the same nonlinear behavior. The response decreased slightly, with an increase in temperature from 250 °C to 300 °C when the concentration of the gas is less than or equal to 2 ppm (Fig. 4c). However, this variation is higher when the concentration is 3 ppm and the lowest and highest responses can be observed at 300 °C and 350 °C respectively. The sensor's response depends on several factors that include adsorbed oxygen, the rate of adsorption/desorption of gas molecules and the carrier concentration which are temperature dependent [46]. All these factors control the number of charge carriers involved in surface reaction, and thus, the response doesn't follow any specific behavior, and it is material and target gas specific. Nevertheless, it can be observed that there is no significant improvement in the response with an increase in response from 250 °C to 350 °C. Though the drift in the sensor response is higher when the temperature is 250 °C, it can be eliminated using the algorithm describe above. Thus,

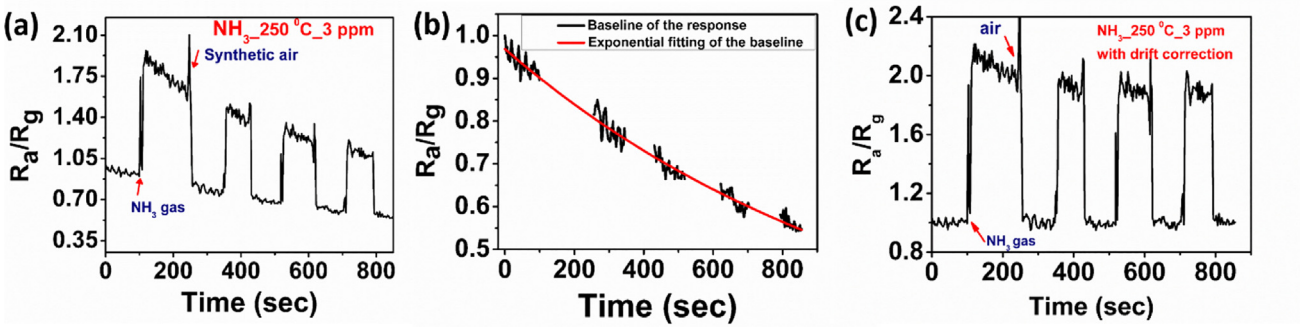

Fig. 3. (a) Repeatability of the sensor for exposure of 4 cycles of 3 ppm ammonia at 250 °C; (b) Exponential fitting of the baseline; (c) Response after baseline correction.

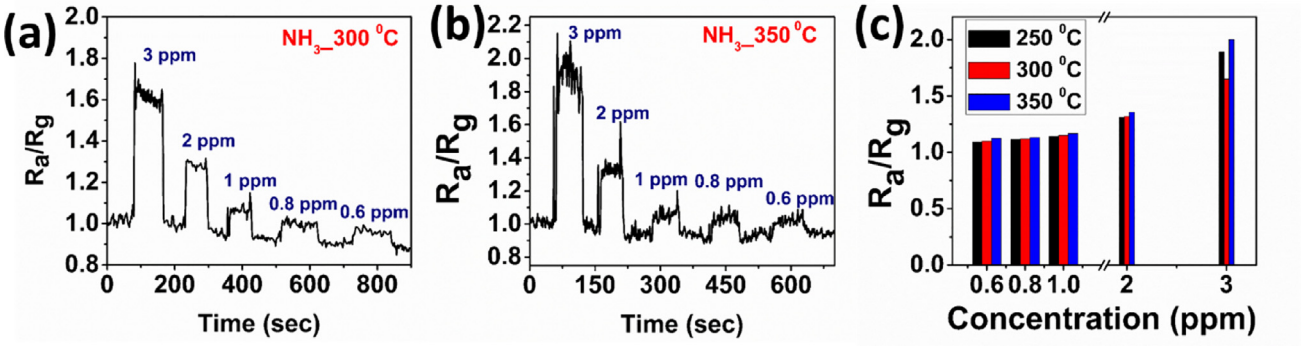

Fig. 4. Dynamic response of sensor at (a) 300 °C and (b) 350 °C; (c) Comparison of response at various temperatures.

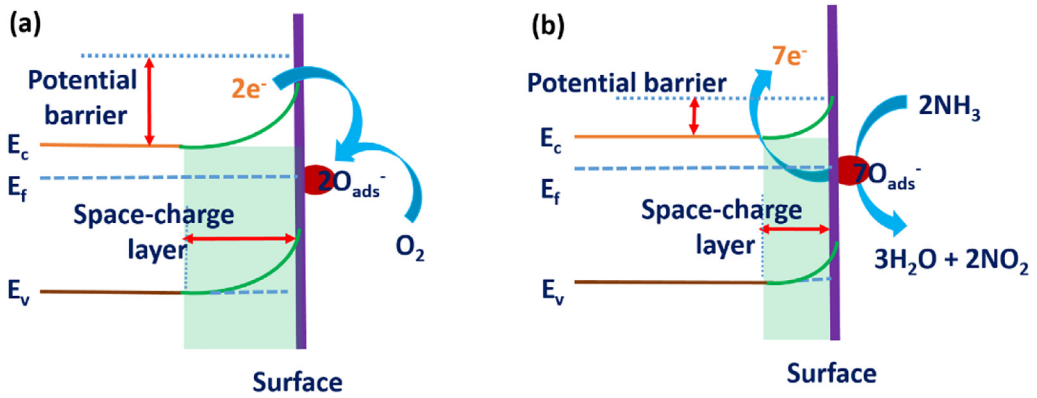

Fig. 5. The principle of gas sensing with ZnO nanoflakes in (a) ambient air and (b) NH_3.

250 °C is the optimum temperature for the operation of this sensor owing to its relatively low power consumption.

3.5. Sensing principle

The sensing principle can be explained using adsorption–desorption of analyte gas on semiconductor metal oxide [47,48]. It involves two steps:

(1) Oxygen molecules in the environment adsorb on ZnO ((1)-(2)) and immobilize the conduction band (CB) electrons on the surface, and consequently, a depletion layer is formed as shown in Fig. 5a.

$$O_{2(gas)} \leftrightarrow O_{2(ads)} \quad (8)$$

$$O_{2(ads)} + 2e^- \rightarrow 2O^-_{(ads)} \quad (9)$$

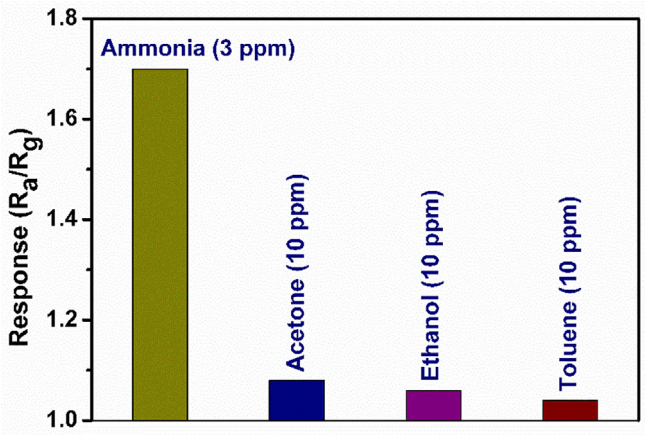

Fig. 6. Selectivity of the sensor against other volatile organic compounds.

Table 2
Comparison of the proposed sensor with the literature.

Material	Operating Temperature (°C)	Concentration (ppm)	Response (%)	Response Time (s)	Recovery Time (s)	Reversible?	Reference
Carbon Nanotubes	RT	100	~25	>300	>300	No	[9]
MoS_2	RT	1000	~80	<100	>100	No	[10]
Graphene	RT	25,000	~10	>1800	>200	No	[11]
Graphene	RT	160	~8	~50	NA	No	[12]
MnO_2 nanofibers	RT	100	~20	~200	~100	Yes	[13]
ZnO thin film	150	600	~57	~120	~600	Yes	[14]
NiO thin film	150	1000	~316	15 @ 10 ppm	~50 @ 10 ppm	Yes	[15]
ZnO nanorods	300	35	~300	<180 @ 10 ppm	<180 @ 10 ppm	Not Reported	[16]
ZnO nano particles	100	46	~3.96	38	158	Yes	[17]
ZnO tapers	RT	25	~3	49	19	Yes	[18]
ZnO nanowalls	RT	25	~1.5	54	23	Yes	[18]
ZnO nanowires	RT	50	~65	28	29	Yes	[19]
ZnO nanorods	RT	25	~1	64	28	Yes	[20]
ZnO/Polypyrrole	RT	1000	~36.1	5	600	Yes	[21]
Cu doped ZnO	RT	100	~30	13	33	Yes	[22]
rGO/ZnO nanowire	RT	1	~7.2	50	200	Yes	[23]
ZnO nanoflakes	250	3	~80	3–15	5–14	Yes	This work

(2) Ammonia reacts with sorbed oxygen ions and releases the electrons back to CB of ZnO. As a result, depletion width and subsequently, barrier potential will be reduced (Fig. 5b) and the conductivity of the sensor increases.

$$2NH_3 + 7O^-_{(ads)} \rightarrow 3H_2O + 2NO_2 + 7e^- \quad (10)$$

Thus, the introduction of the ammonia gas increases the conductivity, and its removal reduces the conductivity as observed earlier.

3.6. Cross-sensitivity of the sensor

To observe the cross-sensitivity of the sensor to other volatile organic compounds (VOC), it was exposed to 10 ppm of acetone, ethanol, and toluene and compared the sensor response with that of 3 ppm ammonia. The response of the sensor to other VOCs is very low even when their concentration is more than three times higher compared to that of ammonia as shown in Fig. 6. Thus the sensor can be used to detect the ammonia selectively at workplace where the presence of other VOCs is possible. As long as the cumulative concentration of other VOCs is less than 10 ppm, it can easily detect ammonia. However, we have to use array of sensors and artificial intelligence to quantify the concentration of each individual gas if the concentration of the mixed VOCs is much higher. The response of the sensor is compared with other metal oxides including ZnO and other emerging materials and highlighted the advantage of this sensor compared to others as depicted in Table 2. For the practical utilization of the gas sensor, it should be highly sensitive, ultra-fast responsive, and yet reversible. We can observe that the other sensors lack at least one of the above features. The proposed sensor has all these features and outperforms all other sensors when we consider this aspect.

4. Conclusion

In summary, 2D ZnO nanoflakes synthesized at low temperature were utilized to implement an NH_3 gas sensor. The sensor showed a nonlinear response in the range of 600 ppb to 3 ppm NH_3 at 250 °C. It exhibited a maximum response of 80% as well as rapid response and recovery (sub-15 s). Further, the baseline drift of the sensor was corrected using a simple and novel division based baseline manipulation technique. Most of the highly sensitive and ultra-fast sensors are unstable, and the baseline varies significantly with time and thus are not useful in real time applications. In such cases, the method we proposed will solve the baseline drift problem, and it is possible to develop the sensors with superior response characteristics. The excellent response of the reported sensor at 250 °C finds diverse applications where all the features, including high sensitivity, reversibility, and ultra-fast response, are critical.

Declaration of Competing Interest

The authors declare that they have no known competing financial interests or personal relationships that could have appeared to influence the work reported in this paper.

References

[1] European Food Safety Authority, Health risk of ammonium released from water filters, EFSA J. 10 (2012) 2918, https://doi.org/10.2903/j.efsa.2012.2918.
[2] S. Naseem, A.J. King, Ammonia production in poultry houses can affect health of humans, birds, and the environment—techniques for its reduction during poultry production, Environ. Sci. Pollut. Res. 25 (2018) 15269–15293, https://doi.org/10.1007/s11356-018-2018-y.
[3] M.J. Fedoruk, R. Bronstein, B.D. Kerger, Ammonia exposure and hazard assessment for selected household cleaning product uses, J. Expo. Anal. Environ. Epidemiol. 15 (2005) 534, https://doi.org/10.1038/sj.jea.7500431.
[4] M.D.H. Rahman, M. Bråtveit, B.E. Moen, Exposure to ammonia and acute respiratory effects in a urea fertilizer factory, Int. J. Occup. Environ. Health. 13 (2007) 153–159, https://doi.org/10.1179/oeh.2007.13.2.153.
[5] Toxic FAQ sheet for ammonia, Agency Toxic Substances Disease 298 Registry, Atlanta, GA, USA, Tech. Rep. CAS 7664-41-7, 2004.
[6] K. Lokesh, G. Kavitha, E. Manikandan, G.K. Mani, K. Kaviyarasu, J.B.B. Rayappan, R. Ladchumananandasivam, J.S. Aanand, M. Jayachandran, M. Maaza, Effective ammonia detection using n-ZnO/p-NiO heterostructured nanofibers, IEEE Sens. J. 16 (2016) 2477–2483, https://doi.org/10.1109/JSEN.2016.2517085.
[7] S. Li, S. Chen, B. Zhuo, Q. Li, W. Liu, X. Guo, Flexible ammonia sensor based on PEDOT:PSS/silver nanowire composite film for meat freshness monitoring, IEEE Electron Device Lett. 38 (2017) 975–978, https://doi.org/10.1109/LED.2017.2701879.
[8] S. Kanaparthi, S.G. Singh, Solvent-free fabrication of a room temperature ammonia gas sensor by frictional deposition of a conducting polymer on paper, Org. Electron. 68 (2019) 108–112, https://doi.org/10.1016/j.orgel.2019.01.053.
[9] A.G. Bannov, O. Jašek, A. Manakhov, M. Márik, D. Nečas, L. Zajíčková, High-performance ammonia gas sensors based on plasma treated carbon nanostructures, IEEE Sens. J. 17 (2017) 1964–1970, https://doi.org/10.1109/JSEN.2017.2656122.
[10] D.J. Late, Y.-K. Huang, B. Liu, J. Acharya, S.N. Shirodkar, J. Luo, A. Yan, D. Charles, U.V. Waghmare, V.P. Dravid, C.N.R. Rao, Sensing behavior of atomically thin-layered MoS2 transistors, ACS Nano. 7 (2013) 4879–4891, https://doi.org/10.1021/nn400026u.
[11] A.R. Cadore, E. Mania, A.B. Alencar, N.P. Rezende, S. de Oliveira, K. Watanabe, T. Taniguchi, H. Chacham, L.C. Campos, R.G. Lacerda, Enhancing the response of NH3 graphene-sensors by using devices with different graphene-substrate distances, Sensors Actuators B Chem. 266 (2018) 438–446, https://doi.org/10.1016/j.snb.2018.03.164.
[12] C. Mackin, V. Schroeder, A. Zurutuza, C. Su, J. Kong, T.M. Swager, T. Palacios, Chemiresistive graphene sensors for ammonia detection, ACS Appl. Mater. Interfaces. 10 (2018) 16169–16176, https://doi.org/10.1021/acsami.8b00853.

[13] R. Kumar, R. Kumar, N. Kushwaha, J. Mittal, Ammonia gas sensing using thin film of MnO_2 nanofibers, IEEE Sens. J. 16 (2016) 4691–4695, https://doi.org/10.1109/JSEN.2016.2550079.
[14] C.-F. Li, C.-Y. Hsu, Y.-Y. Li, NH_3 sensing properties of ZnO thin films prepared via sol–gel method, J. Alloys Compd. 606 (2014) 27–31, https://doi.org/10.1016/j.jallcom.2014.03.120.
[15] P. Chou, H. Chen, I. Liu, C. Chen, J. Liou, K. Hsu, W. Liu, on the ammonia gas sensing performance of a RF sputtered NiO thin-film sensor, IEEE Sens. J. 15 (2015) 3711–3715, https://doi.org/10.1109/JSEN.2015.2391286.
[16] T. Chen, H. Chen, C. Hsu, C. Huang, J. Wu, P. Chou, W. Liu, ZnO-nanorod-based ammonia gas sensors with underlying Pt/Cr interdigitated electrodes, IEEE Electron Device Lett. 33 (2012) 1486–1488, https://doi.org/10.1109/LED.2012.2208729.
[17] I. Rawal, Facial synthesis of hexagonal metal oxide nanoparticles for low temperature ammonia gas sensing applications, RSC Adv. 5 (2015) 4135–4142, https://doi.org/10.1039/C4RA12747A.
[18] M. Chitra, K. Uthayarani, N. Rajasekaran, N. Neelakandeswari, E.K. Girija, D.P. Padiyan, Rice husk templated mesoporous ZnO nanostructures for ethanol sensing at room temperature, Chin. Phys. Lett. 32 (2015) 78101, https://doi.org/10.1088/0256-307x/32/7/078101.
[19] N. Kumar, A.K. Srivastava, R. Nath, B.K. Gupta, G.D. Varma, Probing the highly efficient room temperature ammonia gas sensing properties of a luminescent ZnO nanowire array prepared via an AAO-assisted template route, Dalt. Trans. 43 (2014) 5713–5720, https://doi.org/10.1039/C3DT53305K.
[20] P. Sundara Venkatesh, P. Dharmaraj, V. Purushothaman, V. Ramakrishnan, K. Jeganathan, Point defects assisted NH3 gas sensing properties in ZnO nanostructures, Sensors Actuators B Chem. 212 (2015) 10–17, https://doi.org/10.1016/j.snb.2015.01.070.
[21] P. Patil, G. Gaikwad, D.R. Patil, J. Naik, Synthesis of 1-D ZnO nanorods and polypyrrole/1-D ZnO nanocomposites for photocatalysis and gas sensor applications, Bull. Mater. Sci. 39 (2016) 655–665, https://doi.org/10.1007/s12034-016-1208-9.
[22] G.H. Mhlongo, K. Shingange, Z.P. Tshabalala, B.P. Dhonge, F.A. Mahmoud, B.W. Mwakikunga, D.E. Motaung, Room temperature ferromagnetism and gas sensing in ZnO nanostructures: Influence of intrinsic defects and Mn Co, Cu doping, Appl. Surf. Sci. 390 (2016) 804–815, https://doi.org/10.1016/j.apsusc.2016.08.138.
[23] Z. Sun, D. Huang, Z. Yang, X. Li, N. Hu, C. Yang, H. Wei, G. Yin, D. He, Y. Zhang, ZnO nanowire-reduced graphene oxide hybrid based portable NH3 gas sensing electron device, IEEE Electron Device Lett. 36 (2015) 1376–1379, https://doi.org/10.1109/LED.2015.2496177.
[24] S. Kanaparthi, S.G. Singh, Chemiresistive sensor based on zinc oxide nanoflakes for CO2 detection, ACS Appl. Nano Mater. 2 (2019) 700–706, https://doi.org/10.1021/acsanm.8b01763.
[25] P. Raizada, A. Sudhaik, P. Singh, Photocatalytic water decontamination using graphene and ZnO coupled photocatalysts: A review, Mater. Sci. Energy Technol. 2 (2019) 509–525, https://doi.org/10.1016/j.mset.2019.04.007.
[26] R.N. Radkar, B.A. Bhanvase, D.P. Barai, S.H. Sonawane, Intensified convective heat transfer using ZnO nanofluids in heat exchanger with helical coiled geometry at constant wall temperature, Mater. Sci. Energy Technol. 2 (2019) 161–170, https://doi.org/10.1016/j.mset.2019.01.007.
[27] A. Mohamed Ibraheem, J. Kamalakkannan, Sustainable Scientific Advancements modified Ag2O-ZnO thin films characterization and application of photocatalytic purification of carcinogenic dye in deionizer water and contaminated sea water solutions and Synthetic, Natural based Dye-Sensitized, Solar Cells, Mater. Sci. Energy Technol. 3 (2020) 183–192, https://doi.org/10.1016/j.mset.2019.09.010.
[28] K.A. Adegoke, M. Iqbal, H. Louis, O.S. Bello, Synthesis, characterization and application of CdS/ZnO nanorod heterostructure for the photodegradation of Rhodamine B dye, Mater. Sci. Energy Technol. 2 (2019) 329–336, https://doi.org/10.1016/j.mset.2019.02.008.
[29] M.H. Farooq, I. Aslam, H.S. Anam, M. Tanveer, Z. Ali, U. Ghani, R. Boddula, Improved photocatalytic performance of reduced zinc oxide (ZnO) novel morphology of astray like microstructure under solar light irradiation, Mater. Sci. Energy Technol. 2 (2019) 181–186, https://doi.org/10.1016/j.mset.2019.01.005.
[30] H.P. Uskaikar, N.P. Shetti, S.D. Bukkitgar, S.J. Malode, N.V. Jamakandi, T.M. Manu, Applications of zinc oxide nanoparticles as an electrode modifier for ambroxol, Mater. Today Proc. 18 (2019) 963–967, https://doi.org/10.1016/j.matpr.2019.06.533.
[31] A.B. Bandi, N.P. Shetti, S.J. Malode, S.D. Bukkitgar, R.M. Kulkarni, Electroanalysis of 1,3–dimethylexanthine at zinc oxide nanoparticles modified electrode, Mater. Today Proc. 18 (2019) 590–595, https://doi.org/10.1016/j.matpr.2019.06.452.
[32] S.D. Bukkitgar, N.P. Shetti, R.M. Kulkarni, Construction of nanoparticles composite sensor for atorvastatin and its determination in pharmaceutical and urine samples, Sensors Actuators B Chem. 255 (2018) 1462–1470, https://doi.org/10.1016/j.snb.2017.08.150.
[33] S.D. Bukkitgar, N.P. Shetti, R.M. Kulkarni, K.R. Reddy, S.S. Shukla, V.S. Saji, T.M. Aminabhavi, Electro-catalytic behavior of Mg-doped ZnO nano-flakes for oxidation of anti-inflammatory drug, J. Electrochem. Soc. 166 (2019) B3072–B3078, https://doi.org/10.1149/2.0131909jes.
[34] N.P. Shetti, S.D. Bukkitgar, K.R. Reddy, C.V. Reddy, T.M. Aminabhavi, ZnO-based nanostructured electrodes for electrochemical sensors and biosensors in biomedical applications, Biosens. Bioelectron. 141 (2019), https://doi.org/10.1016/j.bios.2019.111417 111417.
[35] R. Li, L. Wang, D. Kong, L. Yin, Recent progress on biodegradable materials and transient electronics, Bioact. Mater. 3 (2018) 322–333, https://doi.org/10.1016/j.bioactmat.2017.12.001.
[36] J. Li, S. Sathasivam, A. Taylor, C.J. Carmalt, I.P. Parkin, Single step route to highly transparent, conductive and hazy aluminium doped zinc oxide films, RSC Adv. 8 (2018) 42300–42307, https://doi.org/10.1039/C8RA09338E.
[37] R. Vittal, K.-C. Ho, Zinc oxide based dye-sensitized solar cells: A review, Renew. Sustain. Energy Rev. 70 (2017) 920–935, https://doi.org/10.1016/j.rser.2016.11.273.
[38] B. Deka Boruah, Zinc oxide ultraviolet photodetectors: rapid progress from conventional to self-powered photodetectors, Nanoscale Adv. 1 (2019) 2059–2085, https://doi.org/10.1039/C9NA00130A.
[39] A. Gurlo, N. Bârsan, M. Ivanovskaya, U. Weimar, W. Göpel, In2O3 and MoO3–In2O3 thin film semiconductor sensors: interaction with NO2 and O3, Sensors Actuators B Chem. 47 (1998) 92–99, https://doi.org/10.1016/S0925-4005(98)00033-1.
[40] J.X. Wang, X.W. Sun, H. Huang, Y.C. Lee, O.K. Tan, M.B. Yu, G.Q. Lo, D.L. Kwong, A two-step hydrothermally grown ZnO microtube array for CO gas sensing, Appl. Phys. A 88 (2007) 611–615, https://doi.org/10.1007/s00339-007-4076-8.
[41] K. Mukherjee, A.P.S. Gaur, S.B. Majumder, Investigations on irreversible- and reversible-type gas sensing for ZnO and $Mg_{0.5}$ $Zn_{0.5}$ Fe_2 O_4 chemi-resistive sensors, J. Phys. D. Appl. Phys. 45 (2012) 505306, https://doi.org/10.1088/0022-3727/45/50/505306.
[42] M. Sinha, R. Mahapatra, B. Mondal, T. Maruyama, R. Ghosh, Ultrafast and reversible gas-sensing properties of ZnO nanowire arrays grown by hydrothermal technique, J. Phys. Chem. C. 120 (2016) 3019–3025, https://doi.org/10.1021/acs.jpcc.5b11012.
[43] B. Kamp, R. Merkle, J. Maier, Chemical diffusion of oxygen in tin dioxide, Sensors Actuators B Chem. 77 (2001) 534–542, https://doi.org/10.1016/S0925-4005(01)00694-3.
[44] R.K. Sharma, P.C.H. Chan, Z. Tang, G. Yan, I.-M. Hsing, J.K.O. Sin, Investigation of stability and reliability of tin oxide thin-film for integrated micro-machined gas sensor devices, Sensors Actuators B Chem. 81 (2001) 9–16, https://doi.org/10.1016/S0925-4005(01)00920-0.
[45] S. Di Carlo, M. Falasconi, Drift correction methods for gas chemical sensors, in: W. Wang (Ed.), Artificial Olfaction Systems: Techniques and Challenges, InTech, New York, 2012, pp. 305–326, https://doi.org/10.5772/33411.
[46] X. Wang, F. Sun, Y. Duan, Z. Yin, W. Luo, Y. Huang, J. Chen, Highly sensitive, temperature-dependent gas sensor based on hierarchical ZnO nanorod arrays, J. Mater. Chem. C. 3 (2015) 11397–11405, https://doi.org/10.1039/C5TC02187A.
[47] A. Ponzoni, C. Baratto, N. Cattabiani, M. Falasconi, V. Galstyan, E. Nunez-Carmona, F. Rigoni, V. Sberveglieri, G. Zambotti, D. Zappa, Metal oxide gas sensors, a survey of selectivity issues addressed at the SENSOR Lab, Brescia (Italy), Sensors 17 (2017) 714, https://doi.org/10.3390/s17040714.
[48] B.T. Marquis, J.F. Vetelino, A semiconducting metal oxide sensor array for the detection of NOx and NH_3, Sensors Actuators B Chem. 77 (2001) 100–110.